Electrostatic Effects in DNA Bending by GCN4 Mutants†

Juliane K. Strauss-Soukup‡,§ and L. James Maher, III*,§

Department of Biochemistry and Molecular Biology and Eppley Institute for Research in Cancer and Allied Diseases, University of Nebraska Medical Center, Omaha, Nebraska 68198, and Department of Biochemistry and Molecular Biology, Mayo Foundation, Rochester, Minnesota 55905

Received August 28, 1997; Revised Manuscript Received November 4, 1997

ABSTRACT: DNA architecture has been shown to be important for cellular processes such as activation of transcription, recombination, and replication. Many proteins reconfigure the shape of duplex DNA upon binding. Previous experiments have shown that some members of the eukaryotic bZIP family of DNA binding proteins appear to bend DNA, while others do not. We are exploring the role of electrostatic effects in DNA bending by bZIP proteins. The yeast bZIP transcription factor GCN4 does not induce DNA bending *in vitro*. Previously we substituted basic residues for three neutral amino acids in GCN4 to produce a GCN4 derivative that bends DNA by ∼15°. This result is consistent with a model of induced DNA bending wherein excess positive charge in proximity to one face of the double helix neutralizes local phosphate diester anions resulting in a laterally-asymmetric charge distribution along the DNA. Such an unbalanced charge distribution can result in collapse of the DNA toward the neutralized surface. We now present a more comprehensive analysis of electrostatic effects in DNA bending by GCN4 derivatives. It is shown that the direction and extent of DNA bending by these derivatives are a linear function of the charges of the amino acids adjacent to the basic domain of the protein. This relation holds over the charge range +6 (16° bend toward the minor groove) to −6 (25° bend toward the major groove).

The assembly of macromolecular complexes involving multiple proteins bound at specific DNA sites allows processing of the information encoded in DNA. In order for proteins to interact with one another during assembly of such nucleoprotein complexes, the distance between protein binding sites must often be shortened. Therefore, intrinsic DNA curvature and protein-induced DNA bending presumably play significant roles in the functional architecture of promoters (*1*−*4*). In many cases, protein binding has been shown to allow reconfiguration of the double helix and subsequent activation of transcription. For example, the ability of catabolite activator protein (CAP)[1] to induce a ∼90° bend in duplex DNA is thought to allow productive interactions between CAP and the basal transcription machinery (*5*). In addition to CAP, many other proteins induce DNA bending *in vitro*. For example, the TATA binding protein (TBP) is observed to bend duplex DNA by ∼90° in solution (*6*, *7*) and in crystals (*8*, *9*).

Some bZIP proteins, such as the Jun−Fos heterodimer, also appear to induce DNA bending (*10*, *11*) although controversy exists on this point (*12*−*14*). Proteins of the bZIP family contain conserved leucine zipper and basic domains that enable them to dimerize and bind DNA (*15*, *16*). The basic region is a continuous α helix that contacts base pairs within the major groove of the DNA recognition site (e.g., 5′-ATGACTCAT in the present study). The leucine zipper stabilizes a coiled-coil of α helices common to the many combinations of homo- and heterodimers observed among bZIP family members.

Although a number of bZIP proteins appear to induce DNA bending, it is interesting that some family members do not (*17*). Further analysis has suggested that the ability of bZIP proteins to induce DNA bending depends on the identities of the dimer partners. In addition, three amino acids positioned just N-terminal to the basic region may be particularly important (Figure 1). It has been noted that the presence of basic residues in these positions correlates with apparent DNA bending away from the leucine zipper in the resulting complexes (*17*−*21*). This observation suggests that cationic amino acids in these proteins contact one face of the DNA and interact with the negatively charged phosphate diester backbone. In light of our previous studies on DNA bending by asymmetric phosphate neutralization (*22*−*24*), we have been intrigued by the possible role of these residues in DNA bending by bZIP proteins.

GCN4 is a yeast bZIP protein that forms homodimers which do not appear to induce DNA bending (*25*). GCN4

† This work was supported by the Mayo Foundation and NIH Grants GM47814 and GM54411 to L.J.M. and by a University of Nebraska Medical Center Regents Fellowship to J.K.S.-S. L.J.M. is a Harold W. Siebens Research Scholar.

* To whom correspondence should be addressed at the Department of Biochemistry and Molecular Biology, Mayo Foundation, Guggenheim 16, 200 First St., SW, Rochester, MN 55905. Email: maher@mayo.edu. Telephone: 507-284-9041. FAX: 507-284-2053.

‡ University of Nebraska Medical Center.

§ Mayo Foundation.

[1] Abbreviations: CAP, catabolite activator protein; TBP, TATA-box binding protein; bZIP, basic zipper; IPTG, isopropyl β-D-thiogalactopyranoside; Tris-HCl, 2-amino-2-(hydroxymethyl)-1,3-propanediol hydrochloride; EDTA, ethylenediaminetetraacetic acid; bp, base pair(s); SDS, sodium dodecyl sulfate; DTT, dithiothreitol; NP-40, tergitol NP-40 (nonylphenoxypolyethoxyethanol); TBE, Tris−borate, EDTA.

S0006-2960(97)02146-6 CCC: $15.00
Published on Web 01/03/1998

contains the neutral amino acids proline-alanine-alanine (PAA) at the positions that have been suggested to be important for DNA bending (Figure 1B). A testable implication is that substitution of charged amino acids at these positions might induce DNA bending. Furthermore, cationic amino acids are predicted to induce DNA bending toward the neutralized surface, while anionic amino acids are expected to induce DNA bending in the opposite direction (toward the less negatively charged surface). We describe experiments that confirm these hypotheses.

MATERIALS AND METHODS

Oligonucleotides. Oligonucleotides were synthesized on an ABI Model 394 instrument using standard procedures. Oligonucleotides were cleaved and deprotected in hot ammonia and purified by denaturing polyacrylamide gel electrophoresis, eluted from gel slices, and desalted using C_{18} reverse phase cartridges. Oligonucleotide concentrations were determined at 260 nm using molar extinction coefficients (M^{-1} cm^{-1}) of 15 400 (A), 11 700 (G), 7300 (C), and 8800 (T) assuming no hypochromicity.

Plasmids. Plasmid pJ013 encodes the basic and zipper regions of GCN4 [amino acids 226−281 (*26*)] subcloned into pET3b (*27*). Plasmids pJT170-2 through pJT170-9 were used as standards in phasing analyses (*28*). This series of plasmids contains increasing numbers of phased A_6 tracts. Plasmids pDP-AP-1−21, −23, −26, −28, and −30 (*19*) were used to generate phasing probes (see below). GCN4 mutants were created by digesting pJ013 with *Nde*I and *Bss*HII. Oligonucleotides specifying the mutated amino acids were annealed in a 1:1 ratio. The resulting synthetic duplexes were ligated between the *Nde*I and *Bss*HII sites of pJ013 to create plasmids encoding mutant GCN4 derivatives.

Bacterial Extracts Containing Recombinant GCN4 Derivatives. Plasmid pJ013 expressing the bZIP domain of wild-type GCN4 or plasmids expressing mutant GCN4 derivatives were transformed into *Escherichia coli* BL21-(DE3) cells. Cultures were grown to log phase ($A_{600} \sim 0.6$) at 37 °C, IPTG was added to a final concentration of 1 mM, and cells were grown an additional 3 h (*27*). Cells (from 3 mL of culture) were harvested by centrifugation, and the cell pellet was resuspended in extraction buffer (500 μL; 200 mM Tris-HCl, pH 8.0, 10 mM $MgCl_2$, 1 mM EDTA, 7 mM β-mercaptoethanol) and sonicated (Fisher Scientific) on ice for 1 min at a setting of 10 W (*29*). After centrifugation for 30 min (4 °C, 12000*g*), aliquots of the clarified supernatant were frozen at −80 °C.

Preparation of DNA Duplex Probes. Probes for phasing analysis were prepared by PCR from plasmids pDP-AP-1−21, −23, −26, −28, and −30 as previously described (*21*). Pairs of curved DNA standards containing different numbers of phased A_6 tracts at either the center or one terminus of each fragment were prepared by *Nhe*I and *Bam*HI cleavage of plasmids pJT170-2 through pJT170-9 (*28*). The resulting ∼400 bp duplex DNA fragments were purified and radiolabeled as previously described (*21*).

Western Blot Analysis. Protein concentrations were determined using the Bio-Rad (Bradford) assay with detection at 595 nm. Ten micrograms of total protein from each extract was separated on 10−20% SDS−polyacrylamide gels in tricine buffer and transferred onto nitrocellulose. Blocking, antibody incubations, and fluorescent detection were performed as previously described (*21*).

Electrophoretic Gel Mobility Shift Assays. Binding reactions were performed by incubation of the indicated extract (0.25−5 μL) with 1 μL of radiolabeled, duplex DNA probes (AP-1−21, −23, −26, −28, or −30; see above) in a final reaction mixture containing phosphate-buffered saline (2.7 mM KCl, 137 mM NaCl, 4.3 mM Na_2HPO_4, 1.4 mM KH_2PO_4 pH 7.3), 5% glycerol, 1 mM EDTA, 1 mM DTT, 0.05% NP-40, and 26−36 μg/mL poly(dI·dC) as described by Paolella et al. (*19*). The amount of bacterial extract was chosen empirically to partially saturate the labeled DNA probe. Binding reactions were incubated on ice for 30 min. Free and protein-bound DNA probes were resolved by nondenaturing 8% polyacrylamide gel electrophoresis [29:1 acrylamide:bis(acrylamide)] in 0.5× TBE buffer for 20 h at 4 °C (12 $V \cdot cm^{-1}$). Dried gels were analyzed by storage phosphor technology.

Phasing Analysis Calculations. Mobilities (μ) of free and bound DNA fragments were taken as the distance (mm) from the center of the electrophoresis well to the center of the band corresponding to free or protein-complexed DNA and were normalized to the average mobility of each set of probes to give relative mobility:

$$\mu_{rel} = \mu/\bar{\mu} \qquad (1)$$

where $\bar{\mu}$ corresponds to the average value of μ for a set of phasing probes. Values of μ_{rel} were then plotted against the phasing spacing (distance in bp between the center of the AP-1 site and the center of the A_5 tract array) for fitting to the phasing function:

$$\mu_{rel} = (A_{PH}/2)\{\cos[2\pi(S - S_T)/P_{PH}]\} + 1 \qquad (2)$$

where μ_{rel} is the relative mobility of the free or protein-complexed DNA, S is the phasing spacer length (bp), P_{PH} is the phasing period (set at 10.5 bp/turn), S_T is the trans spacer length (bp; the length where the intrinsic and protein-induced bends are predicted to most nearly cancel giving maximal mobility), and A_{PH} is the amplitude of the phasing function (*30*). The value of A_{PH} was estimated by curve fitting and is related to the magnitude of the directed bend. Curve fitting was performed by the least squares method using KaleidaGraph software (Synergy Software Co.). The directed DNA bend angle, α_β, was obtained using the relation:

$$\tan(k\alpha_B/2) = (A_{PH}/2)/[\tan(k\alpha_C/2)] \qquad (3)$$

where α_C is the reference bend angle magnitude (54° for three A_{5-6} tracts), and k is empirically determined using the electrophoretic behavior of bending standards. To determine k, the mobilities of the bending standards were fit to the function:

$$A_{CP} = 1 - \cos(k\alpha/2) \qquad (4)$$

where α is the angle due to the A_{5-6} tracts, and A_{CP} is the amplitude of the circular permutation function reflecting the magnitude of the DNA distortion (*30*). The value A_{CP} is given by

$$A_{CP} = |(\mu_{center}/\mu_{end}) - 1| \qquad (5)$$

Sequence at XXX	Designation	Tripeptide formal charge
KKK	(PAA→KKK)	+3
PKK	(PAA→PKK)	+2
PAK	(PAA→PAK)	+1
PAA	GCN4	0
PAE	(PAA→PAE)	-1
PEE	(PAA→PEE)	-2
EEE	(PAA→EEE)	-3

FIGURE 1: bZIP proteins under investigation. (A) GCN4 homodimer (spheres) bound to the AP-1 DNA sequence [ribbon (*35*)]. Locations of amino acid substitutions are indicated by black spheres and arrows. DNA major (M) and minor (m) grooves at the center of the AP-1 site are indicated. (B) Amino acid sequences of the recombinant GCN4 derivatives studied. Leucines of the zipper heptad repeat are underlined (top). The black box indicates amino acids that were mutated. The resulting sequences, designations, and tripeptide formal charges are indicated below. Charge refers to a monomer, so the charge must be doubled when considering dimeric bZIP proteins. Both wild-type and mutant recombinant proteins also contained the N-terminal sequence MASMTGGQQMGR and the C-terminal sequence KKLESGQ.

where μ_{center} and μ_{end} are mobilities of circularly permuted DNA fragments where phased arrays of A_6 tracts are located at the center or end of the fragment, respectively. The average value of *k* under the present electrophoretic conditions was 1.09.

RESULTS

Design of GCN4 Mutants. Previous experiments have shown that the presence of basic amino acids adjacent to the conserved basic domains of bZIP proteins correlates with electrophoretic behavior that can be interpreted as DNA bending toward the minor groove [i.e., away from the leucine zipper such that the DNA in Figure 1A adopts a "frown" configuration (*17*−*21*)]. The yeast bZIP protein GCN4 contains the sequence PAA adjacent to the basic region, and does not appreciably bend DNA in electrophoretic experiments (*25*). We have shown that mutation of these neutral amino acids to the basic amino acids KRR (as found in Fos) or to KKK induces ∼15° of DNA bending by GCN4 homodimers (*21*). We wished to establish whether variations in the net charge of this tripeptide have systematic effects on DNA bending. We therefore mutated the PAA sequence found in wild type GCN4 to yield combinations of amino acids such that the net charge of this tripeptide region ranged from +3 to −3 (Figure 1).

The effect of amino acid substitutions on protein expression was examined by Western blotting. GCN4 derivatives were expressed in *E. coli* with an N-terminal T7 epitope that is recognized by a monoclonal T7 tag antibody. Chemifluorescence detection allowed estimation of protein levels. GCN4 derivatives were expressed at somewhat reduced levels relative to wild-type GCN4 (Figure 2). The relationship between the different GCN4 derivatives and their levels of expression relative to wild type was as follows: GCN4-(PAA→KKK), ∼38%; GCN4(PAA→PKK), ∼16%; GCN4-(PAA→PAK), ∼21%; GCN4(PAA→PAE), ∼43%; GCN4-(PAA→PEE), ∼35%; and GCN4(PAA→EEE), ∼34%. Besides being expressed at different levels in different crude extracts (Figure 2), the specific binding activities of each mutant form have not been determined in these experiments. As described under Materials and Methods, the amount of bacterial extract was adjusted for each mutant to partially saturate labeled DNA probes in electrophoretic mobility shift assays. Thus, differences in the degrees of probe saturation observed in gel mobility shift assays do not reflect the intrinsic affinities of the various mutants for the AP-1 site.

FIGURE 2: Western blot of crude protein extracts from *E. coli* BL21-(DE3) cells expressing different GCN4 derivatives. Lanes 1 and 6 contain extracts of cells carrying the expression vector alone, lanes 2 and 7 contain extracts expressing the wild-type GCN4 derivative, and lanes 3−5 and 8−10 contain extracts of cells expressing GCN4 with the indicated amino acids substituted for PAA.

Phasing Analysis. Electrophoretic mobility shift assays were employed to study apparent changes in average DNA shape due to both intrinsic DNA curvature and protein-induced DNA bending. Nondenaturing gel electrophoresis was employed to measure DNA shape. We interpreted phase-dependent differences in electrophoretic mobility between molecules of the same length as evidence of DNA bending. DNA fragments used in our phasing analyses contained a protein recognition sequence (i.e., the AP-1 site) and a reference sequence of defined curvature, in this case an array of phased A_5 tracts. Phasing analysis measures the overall DNA shape as the distance between these elements of curvature is altered (*11*, *13*, *19*, *31*). The resulting phase-dependent changes in mobility allow estimation of the magnitude and orientation of a directed bend relative to the intrinsic curvature present in the fragment.

Phasing probes (437−446 bp) used to study DNA bending by GCN4 derivatives were described previously (*21*). In these phasing probes, the AP-1 site (5′-ATGACTCAT) is

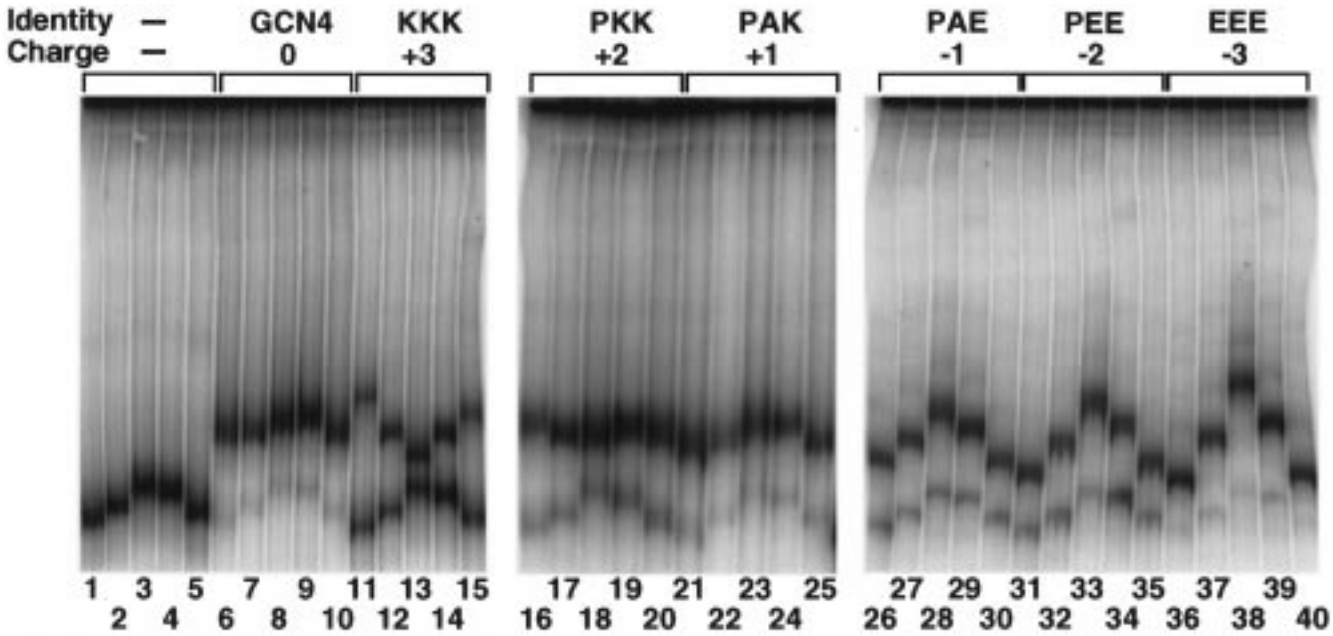

FIGURE 3: Electrophoretic mobility shift assay of GCN4 and GCN4 mutant homodimers bound to phasing analysis probes. Lanes 1−5 contain phasing probes from plasmids pDP-AP-1−21, −23, −26, −28, and −30, respectively, incubated with an extract of *E. coli* cells containing the expression vector alone. Lanes 6−40 contain the same five phasing probes incubated with *E. coli* extracts containing homodimers of wild type GCN4 (lanes 6−10), GCN4(PAA→KKK) (lanes 11−15), GCN4(PAA→PKK) (lanes 16−20), GCN4(PAA→PAK) (lanes 21−25), GCN4(PAA→PAE) (lanes 26−30), GCN4(PAA→PEE) (lanes 31−35), and GCN4(PAA→EEE) (lanes 36−40). The indicated formal charges refer to a monomer, so the charge must be doubled when considering dimeric bZIP proteins.

separated from a 25 bp curved DNA element by a variable linker. The 25 bp curved sequence contains three A_5 tracts with an overall curvature of 54° toward the minor groove (in a reference frame taken to be 0.5 bp 3′ to the central A of the central A_5 tract in the array). The five probes differ only in the length of the variable linker separating the AP-1 site and A_5 tract array.

The AP-1 Site Has Intrinsic Curvature. Lanes 1−5 of Figure 3 depict mobilities of phasing probes incubated with *E. coli* extract lacking GCN4 peptides. The absence of shifted complexes indicates that there are no endogenous *E. coli* proteins that bind to the phasing probes. Slight intrinsic probe curvature in or near the AP-1 site is implied by the different mobilities observed for the five phasings. An estimate of ∼8° intrinsic curvature toward the major groove at the AP-1 site was determined from phasing analysis and the arbitrary assumption that the center of the AP-1 site is the site of curvature (Figure 4; Table 1). This result is in agreement with previous results from our laboratory that estimated this curvature to be ∼7° (*21*).

GCN4 Does Not Bend the AP-1 Site. Binding reactions with labeled AP-1 probes and extract containing wild-type GCN4 protein (basic and zipper regions) resulted in complexes whose mobilities reflected the same DNA curvature pattern as was observed for the free probes (Figure 3, compare lanes 6−10 with lanes 1−5). Analysis of these phasing data suggest a bend angle of ∼5° toward the major groove (Figure 4; Table 1). This value is comparable to the ∼8° intrinsic curvature measured for the unbound AP-1 site, and corresponds to a slight "smile" configuration of the DNA in Figure 1A. Note that the binding data in Figure 3 are qualitative; i.e., it is the relative mobility (rather than the extent of probe saturation) in each complex that is significant (see above).

Table 1: DNA Bending Induced by GCN4 and Mutant Derivatives

bZIP protein	tripeptide formal charge[a]	bend angle (deg)[b]
GCN4(PAA→KKK)	+3	−15.5 ± 1.8
GCN4(PAA→PKK)	+2	−04.3 ± 1.0
GCN4(PAA→PAK)	+1	04.6 ± 1.1
GCN4	0	04.9 ± 0.1
GCN4(PAA→PAE)	−1	14.4 ± 0.8
GCN4(PAA→PEE)	−2	19.0 ± 1.0
GCN4(PAA→EEE)	−3	25.2 ± 1.5

[a] Formal charge of the tripeptide corresponding to PAA in GCN4. Charge refers to a monomer, so the charge must be doubled when considering dimeric bZIP proteins. [b] Based on best fits to phasing eq 2 (Materials and Methods) where bend angle >0 indicates bending toward the DNA major groove; bend angle <0 indicates bending toward the DNA minor groove. In the absence of protein binding, the AP-1 phasing probes displayed intrinsic curvature interpreted as ∼8° toward the major groove at the center of the AP-1 sequence. Data represent average ± standard deviation based on results from three experiments.

GCN4 Mutants Bearing Two or Three Cationic Residues Induce DNA Bending toward the Minor Groove. Three mutant GCN4 derivatives carry a net positive charge in the tripeptide sequence of interest. Binding reactions with labeled AP-1 probes and bacterial extracts containing recombinant GCN4(PAA→KKK) or GCN4(PAA→PKK) proteins produced complexes whose mobilities suggested DNA bending opposite to that measured for free probes or wild-type GCN4−DNA complexes (Figure 3, compare mobility patterns in lanes 11−20 with lanes 1−10; Figure 4; Table 1). In contrast, the mobility pattern for GCN4-(PAA→PAK)−DNA complexes indicates the same DNA curvature observed for free probes and for wild type GCN4−DNA complexes (Figure 3, compare lanes 21−25 with lanes 1−10; Figure 4; Table 1). Thus, for homodimeric GCN4 derivatives, disposition of four or six positively charged

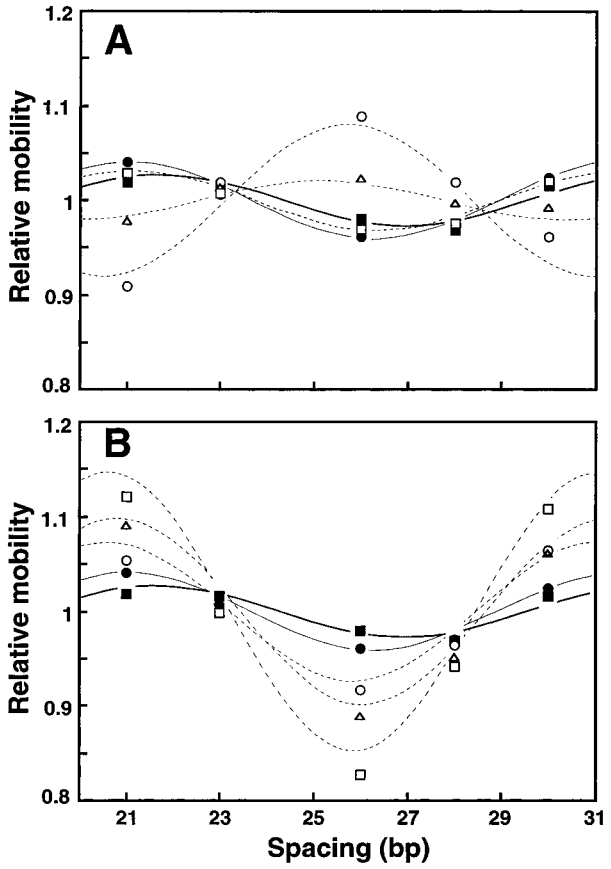

FIGURE 4: Analysis of phasing data. Relative gel mobilities are plotted as a function of the spacing (bp) between the center of the AP-1 site and the center of the A_5 tract array. (A) GCN4 vs derivatives with net positive charge at the tripeptide. Mobilities of free probes (●, thin line) and complexes involving wild-type GCN4 (■, thick line), GCN4(PAA→KKK) (○, dotted line), GCN4-(PAA→PKK) (△, dotted line), and GCN4(PAA→PAK) (□, dotted line) are shown. (B) GCN4 vs derivatives with net negative charge at the tripeptide. Mobilities of free probes (●, thin line) and complexes involving wild-type GCN4 (■, thick line), GCN4-(PAA→PAE) (○, dotted line), GCN4(PAA→PEE) (△, dotted line), and GCN4(PAA→EEE) (□, dotted line) are shown. Both plots depict the calculated best fits of the data to the phasing eq 2 described under Materials and Methods. Data reflect the average from three experiments.

amino acids on one face of the AP-1 site appeared to induce DNA bending toward the neutralized face, whereas no induced bending was observed in the case of two cationic amino acids.

GCN4 Mutants Bearing Anionic Residues Induce DNA Bending Away from the Minor Groove. Binding reactions with labeled AP-1 probes and bacterial extracts containing recombinant GCN4(PAA→PAE), GCN4(PAA→PEE), or GCN4(PAA→EEE) proteins produced complexes whose mobilities suggested DNA bending opposite to that measured for derivatives with cationic tripeptides (Figure 3, compare mobility patterns in lanes 26−40 with lanes 11−25). Quantitative data are summarized in Figure 4 and Table 1. For GCN4 derivatives with formal charges of −3, −2, and −1 within the tripeptide of interest, induced DNA bending toward the major groove was ∼25°, ∼19°, and ∼14°, respectively (note that ∼5° of bending toward the major groove occurs for the wild-type GCN4−DNA complex). As summarized in Table 1, the incremental effect of negative charges is 5−6° per pair of anionic amino acids after the first pair (which alters the bend by 10°), about half the effect seen for pairs of positive charges after the first pair. This asymmetry might reflect a tendency of negatively-charged residues to be deflected further away from the DNA. In this regard, it is perhaps surprising that the first pair of positive charges introduced (PAA→PAK) has no effect since it occurs closest to the DNA.

In summary, these data for homodimeric GCN4 derivatives show that disposition of six, four, or two negatively charged amino acids on one face of the AP-1 site appears to induce DNA bending away from the more negatively charged face.

DISCUSSION

DNA bending by bZIP proteins has been measured using numerous techniques (*12*−*14*, *17*). A comparison of these results has previously been presented (*13*). Controversy surrounds several aspects of these studies. First, some electrophoretic phasing experiments indicate phase-dependent electrophoretic mobilities of bZIP/DNA complexes (*10*, *11*), while others do not (*12*). Subsequent analysis of the difference between these experiments tends to clarify the discrepancies by showing that probe geometry is an important consideration (*13*). In particular, long phasing probes with closely spaced curvature elements were shown to be the most sensitive to DNA bending.

A remaining point of contention is the failure of sensitive ring closure experiments to detect DNA bending induced by the binding of Jun/Fos heterodimers to the AP-1 site (*12*). Though counterarguments have been put forward (*13*), this discrepancy remains unresolved. Others have argued that the entire subject of bZIP-induced DNA bending is physiologically unimportant because of the small bend angles involved (*14*).

This paper measures apparent DNA bending using electrophoretic phasing analysis, and we implicitly assume that the phase-dependent changes in electrophoretic mobility reflect protein-induced DNA bending. Other explanations for our data include: (i) amino acid substitutions in the PAA tripeptide near the amino terminus of GCN4 produce dramatic changes in the structure of the leucine zipper domain, (ii) changes in the sequence of this tripeptide alter its structure in a manner that dramatically changes gel mobility, or (iii) changes in the electrostatic character of the tripeptide sequence alter the rigidity of the protein−DNA complex in some manner that causes phase-dependent changes in electrophoretic mobility. While these alternative explanations are not formally excluded, we favor DNA bending as the most plausible interpretation to account for the proportionality between electric charge at the GCN4 N-terminus and phase-dependent electrophoretic anomalies.

It has previously been hypothesized that electrostatic interactions might explain the different degrees of DNA bending observed for different bZIP proteins (*17*−*21*). Our laboratory has focused on the possible role of asymmetric phosphate neutralization in bZIP-induced DNA bending. Neutralization involves the negatively charged phosphate backbone of duplex DNA and the cationic amino acids of an approaching protein. According to one model (*22*, *32*, *33*), the resulting unbalanced charge distribution along the duplex DNA induces the double helix to collapse toward the neutralized or less negatively charged surface. We (*21*)

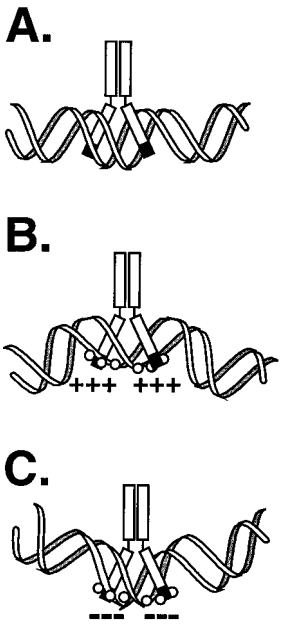

FIGURE 5: Schematic representation of induced DNA bending. (A) Wild-type GCN4 homodimer binding to duplex DNA induces little DNA bending. (B) GCN4 derivatives with cationic tripeptide sequences induce DNA bending toward the minor groove (i.e., toward the neutralized DNA surface). (C) GCN4 derivatives with anionic tripeptide sequences induce DNA bending away from the minor groove (i.e., collapse toward the less negatively charged surface). Note that bend angles are exaggerated for clarity.

and others (*18*, *20*) have observed that substitution of positively charged residues N-terminal to the basic region of the protein induces DNA bending toward the minor groove (i.e., toward the neutralized face). We now extend this result by showing that addition of negatively charged residues at the same positions induces DNA bending in the opposite direction, away from the minor groove (i.e., toward the less negatively charged surface). This result is consistent with the predictions of DNA collapse associated with asymmetric charge distribution. Thus, the asymmetric addition of negative charges increases phosphate repulsions along one DNA face, resulting in a force bending the DNA toward the less negatively charged surface. These results are summarized in Figure 5.

A similar ability of negatively charged amino acids to induce DNA bending by bZIP proteins has been illustrated in previous work by Kerppola and co-workers (*20*, *34*). These authors first showed that small changes in the charge of two amino acids near the amino terminus of monomers in the Jun/Fos heterodimer caused detectable changes in apparent DNA bending (*20*). Indeed, Figure 6 depicts bending data for mutant forms of the Jun/Fos heterodimer (*20*) compared with the present data set for GCN4 mutants. Interestingly, both data sets show similar, roughly linear relationships between peptide charge and DNA bending. We cannot account for this apparent proportionality between charge and deflection angle as it would not be predicted from first principles. Second, these authors presented evidence that the very acidic transactivation domains of Jun and Fos appear to act at a distance (and independent of the DNA binding domains) to alter DNA bending. DNA bending by these proteins appears to involve deflection of the double helix away from the respective anionic transcription activation domains. DNA bending in these studies was reduced in the

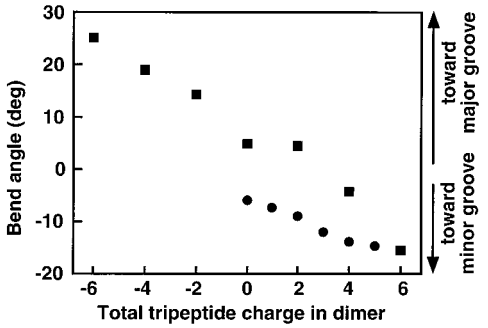

FIGURE 6: Graphical representation of the relation between apparent DNA bend angle and tripeptide formal charge for recombinant GCN4 and GCN4 derivatives (■). The data of Leonard et al. (1997) for mutated derivatives of Jun/Fos are included for comparison (●).

presence of multivalent cations, consistent with an electrostatic contribution to the bending force (*20*, *34*).

Electrostatic effects are again evident in the results of the present DNA bending study. However, distinguishing models based on electrostatic attraction between DNA phosphates and protein side chains vs DNA collapse due to asymmetric charge neutralization is not formally possible based on the present experiments. Likewise, it is difficult to distinguish whether anionic amino acids induce DNA bending by repelling phosphate charges, or induce DNA collapse by creating unbalanced repulsive forces between phosphates. With reference to Figure 1A, the electrostatic forces of amino-terminal amino acids introduced by the binding of a relatively rigid protein may be focused along the anionic DNA backbone flanking the DNA minor groove. In this case, repulsion produced by anionic amino residues in these positions might be envisioned as "clamping" or "pinching" together the deoxyribose−phosphate backbones flanking this minor groove, resulting in its compression (DNA bends "downward"). Similarly, if extra cationic residues of such a rigid protein are present at these positions, they might be predicted to attract phosphates on the DNA backbone, expanding the width of the minor groove (DNA bends "upward"). Insofar as the DNA curvature predicted to result from such direct repulsions or attractions is opposite to what is suggested by our phasing results, a DNA collapse model may be more easily reconciled with the data. Discerning the actual origins of such electrostatic forces is ultimately a goal of "phantom protein" studies in which the degree of DNA collapse due to phosphate neutralization is measured using DNA analogs designed to simulate the electrostatic consequences of protein binding (*22*−*24*).

The DNA binding domain of GCN4 contains numerous conserved basic residues. The shape of DNA does not appear to respond to all of these residues. One possible explanation is that the cationic core of the GCN4 basic region packs into the major groove, immobilizing the double helix so that electrostatic effects on DNA shape are not evident. In contrast, DNA proximal to the basic region (near the added cationic or anionic amino acid residues in this study) may be more flexible and able to respond to laterally asymmetric charge distributions.

This work presents evidence that electrostatic effects explain how bZIP variants differentially alter the structure of DNA upon binding. The data are consistent with a model in which the trajectory of DNA responds to lateral asymmetries in charge density. It will be interesting to determine

if this model applies to induced DNA bending by other proteins. Ultimately, we hope to use these principles to design novel peptides or proteins that bend nucleic acids.

ACKNOWLEDGMENT

We thank B. Mueller-Hill for plasmid pPLc28-bZIP, T. Kerppola for pJT170 plasmids, A. Schepartz and D. Paollela for pDP-AP-1 plasmids, and C. Vinson for pET3b plasmid and helpful discussions. We acknowledge the staff of the Mayo Foundation Molecular Biology Core Facility for excellent oligonucleotide synthesis and DNA sequencing services.

REFERENCES

1. Perez-Martin, J., Rojo, F., and de Lorenzo, V. (1994) *Microbiol. Rev. 58*, 268−290.
2. Perez-Martin, J., and Espinosa, M. (1993) *Science 260*, 805−807.
3. Travers, A. A. (1993) *DNA−Protein Interactions*, Chapman & Hall, London.
4. Zinkel, S. S., and Crothers, D. M. (1991) *J. Mol. Biol. 219*, 201−215.
5. Schultz, S. C., Shields, G. C., and Steitz, T. A. (1991) *Science 253*, 1001−1007.
6. Starr, D. B., Hoopes, B. C., and Hawley, D. K. (1995) *J. Mol. Biol. 250*, 434−446.
7. Parkhurst, K. M., Brenowitz, M., and Parkhurst, L. J. (1996) *Biochemistry 35*, 7459−7465.
8. Kim, Y., Greiger, J. H., Hahn, S., and Sigler, P. B. (1993) *Nature 365*, 512−520.
9. Kim, J. L., Nikilov, D. B., and Burley, S. K. (1993) *Nature 365*, 520−527.
10. Kerppola, T. K., and Curran, T. (1991) *Cell 66*, 317−326.
11. Kerppola, T. K., and Curran, T. (1991) *Science 254*, 1210−1214.
12. Sitlani, A., and Crothers, D. M. (1996) *Proc. Natl. Acad. Sci. U.S.A. 93*, 3248−3252.
13. Kerppola, T. K. (1996) *Proc. Natl. Acad. Sci. U.S.A. 93*, 10117−10112.
14. Hagerman, P. J. (1996) *Proc. Natl. Acad. Sci. U.S.A. 93*, 9993−9996.
15. Landschulz, W. H., Johnson, P. F., and McKnight, S. L. (1988) *Science 240*, 1759−1764.
16. McKnight, S. L. (1991) *Sci. Am. 264*, 54−64.
17. Kerppola, T. K., and Curran, T. (1993) *Mol. Cell. Biol. 13*, 5479−5489.
18. Paolella, D. N., Liu, Y., and Schepartz, A. (1997) *Biochemistry 36*, 10033−10038.
19. Paolella, D. N., Palmer, C. R., and Schepartz, A. (1994) *Science 264*, 1130−1133.
20. Leonard, D. A., Rajaram, N., and Kerppola, T. K. (1997) *Proc. Natl. Acad. Sci. U.S.A. 94*, 4913−4918.
21. Strauss-Soukup, J. K., and Maher, L. J. (1997) *Biochemistry 36*, 10026−10032.
22. Strauss, J. K., and Maher, L. J. (1994) *Science 266*, 1829−1834.
23. Strauss, J. K., Roberts, C., Nelson, M. G., Switzer, C., and Maher, L. J. (1996) *Proc. Natl. Acad. Sci. U.S.A. 93*, 9515−9520.
24. Strauss, J. K., Prakash, T. P., Roberts, C., Switzer, C., and Maher, L. J. (1996) *Chem. Biol. 3*, 671−678.
25. Gartenberg, M. R., Ampe, C., Steitz, T. A., and Crothers, D. M. (1990) *Proc. Natl. Acad. Sci. U.S.A. 87*, 6034−6038.
26. Suckow, M., van Wilcken-Bergmann, B., and Mueller-Hill, B. (1993) *EMBO J. 12*, 1193−2000.
27. Studier, F. W., Rosenberg, A. H., Dunn, J. J., and Dubendorff, J. W. (1990) *Methods Enzymol. 185*, 60−89.
28. Thompson, J. F., and Landy, A. (1988) *Nucleic Acids Res. 16*, 9687−9705.
29. Suckow, M., van Wilcken-Bergmann, B., and Mueller-Hill, B. (1993) *Nucleic Acids Res. 21*, 2081−2086.
30. Kerppola, T. K. (1994) in *Transcription: Mechanisms and Regulation* (Conaway, R. C., & Conaway, J. W., Eds.) Raven Press, Ltd., New York.
31. Zinkel, S. S., and Crothers, D. M. (1987) *Nature 328*, 178−181.
32. Mirzabekov, A. D., and Rich, A. (1979) *Proc. Natl. Acad. Sci. U.S.A. 76*, 1118−1121.
33. Manning, G., Ebralidse, K. K., Mirzabekov, A. D., and Rich, A. (1989) *J. Biomol. Struct. Dyn. 6*, 877−889.
34. Kerppola, T. K., and Curran, T. (1997) *EMBO J. 16*, 2907−2916.
35. Ellenberger, T. E., Brandl, C. J., Struhl, K., and Harrison, S. C. (1992) *Cell 71*, 1223−1237.

BI972146P